

Realtime Health Monitoring of Composite Structures Using FBG Sensors

Author

Okagawa, Shoi, Bernus, Peter, Noran, Ovidiu

Published

2022

Conference Title

IFAC-PapersOnLine

Version

Version of Record (VoR)

DOI

[10.1016/j.ifacol.2022.09.200](https://doi.org/10.1016/j.ifacol.2022.09.200)

Downloaded from

<http://hdl.handle.net/10072/420573>

Griffith Research Online

<https://research-repository.griffith.edu.au>

Realtime Health Monitoring of Composite Structures Using FBG Sensors

Shoi Okagawa*, Peter Bernus**, Ovidiu Noran***

*Griffith University, QLD, Australia (e-mail: sokag99@gmail.com, shoi.okagawa@griffithuni.edu.au).

** Griffith University, QLD, Australia (email: p.bernus@griffith.edu.au)

*** Griffith University, QLD, Australia (email: o.noran@griffith.edu.au)

Abstract: Although composite structures popular in aerospace structures, due to complex failure modes, frequent inspection is required, increasing maintenance costs. Consequently, a structural health monitoring (SHM) system to monitor and pre-emptively detect damage is crucial. The Institute for Integrated and Intelligent Systems (IIIS) and the Advanced Design and Prototyping Technologies Institute (ADaPT) at Griffith University are planning to design and build a real-time SHM system utilizing Fiber Bragg Grating (FBG) sensors to obtain health data and use machine learning for real-time damage classification. We propose an experimental setup to generate ground truth neural network training. This includes methods to obtain data on material condition, an interrogation system for real-time monitoring, and machine learning for damage classification and remaining useful life (RUL) prediction.

Copyright © 2022 The Authors. This is an open access article under the CC BY-NC-ND license (<https://creativecommons.org/licenses/by-nc-nd/4.0/>)

Keywords: Structural Health Monitoring (SHM); Fiber Bragg Grating (FBG); Aerospace

1. INTRODUCTION

This paper is a part of a larger project to design and implement a real-time SHM system for composite materials in aerospace structures. The system consists of three sections (Fig. 1): i) the composite part monitored, the Fiber Bragg grating (FBG) sensor and the interrogator; ii) filter and storage system to identify and store significant features of the system under dynamic load, resulting a real time system model – a ‘digital twin’; iii) the neural network system to identify relevant features (point in time measurements, events, and trends) to obtain situation awareness and prediction capability for decision support.

1.1 Structural health monitoring (SHM)

The Condition-based Maintenance Plus guidebook' (US DoD, 2008) states that operation and support expenses of US DoD weapon systems make up 65~80% of total life cycle cost. The US Air Force developed the Aircraft Structural Integrity Program (ASIP) in the 1970s to conduct schedule-based inspections on airframe structures when internal damage becomes detectable by non-destructive methods (Giurgiutiu, 2014) used regardless of the actual airframe condition, but in most cases no damage is found (Derriso, et al., 2016).

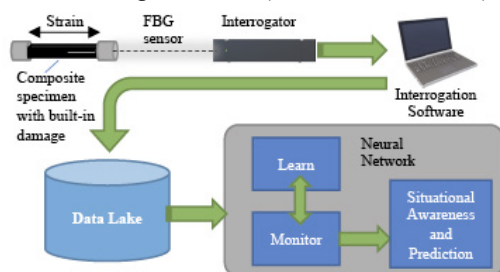


Figure 1. Schematic diagram of the project

Therefore, platforms are removed from service despite being in working condition (Derriso, et al., 2016). In 2007 the DoD implemented a “Condition-Based Maintenance Plus” (CBM+) policy, to decrease maintenance burden, while maintaining safety (Department of Defense, 2008), increasing the focus on advanced material health management technologies (Giurgiutiu, 2014) (Derriso, et al., 2016).

1.2 Fiber Bragg grating sensors

FBGs are made by periodically altering the refractive index of the core of an optical fiber (Werneck, et al., 2013) by inscribing ‘gratings’ inside the fiber. When broadband light is passed through this grating, narrowband light with a specific peak wavelength is reflected (Sahota, et al., 2020). External factors cause the FBG properties to change causing reflected wavelength shift, which is then measured. A diagram of the structure of an FBG sensor is shown in Fig. 2 (Sahota, et al., 2020). Reflected Bragg wavelength λ_B is given by Eq. 1.

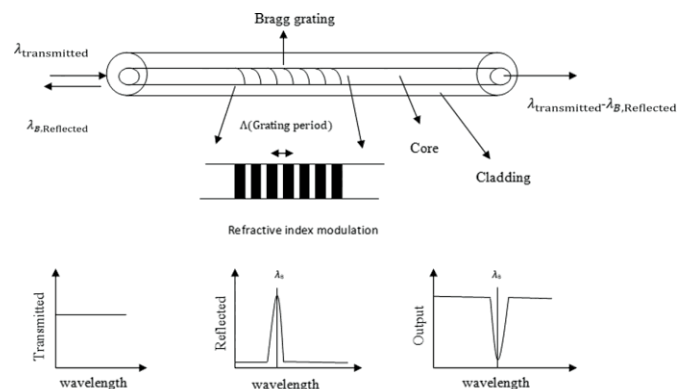


Figure 2. Structure of an FBG sensor (Sahota, et al., 2020)

$$\lambda_B = 2\Lambda n_{eff} \quad (1)$$

where Λ is the grating period (distance between adjacent gratings), and n_{eff} is the effective core refractive index (Werneck, et al., 2013). The two factors FBG sensors can measure directly are strain and temperature. By applying strain on the fiber, the grating period alters, causing change in reflected wavelength. Temperature changes cause a change in effective refractive index, also causing wavelength shift. Utilizing these characteristics, FBGs can be used to measure other physical parameters as well (Werneck, et al., 2013).

1.3 Machine learning classifiers

In traditional machine learning, features must be extracted manually, and a highly knowledgeable individual of the subject is required to train a classifier (Pai, 2020). Deep learning algorithms are designed to be trained without a requiring manual feature identification (Zhang & Wang, 2020), and can be trained without extensive knowledge of the input (Pai, 2020). Training a neural network (NN) with few layers is time consuming, however, training a fully connected many-layer NN requires extensive computation (Kusiak, 2019). Convolutional neural networks (CNN) reduce connectivity between layers (Zhang & Wang, 2020), requiring less data pre-processing (Kusiak, 2019).

2. STATE OF THE ART REVIEW

2.1 Temperature compensation

The operating temperatures of aerospace structures can range from around -55°C to 40°C (Alam, et al., 2019). One major problem with FBG sensors is that they provide one response to both strain and temperature (Tian, et al., 2005). This makes it difficult to measure the parameter of interest making signal response interpretation difficult (Sahota, et al., 2020), thus temperature compensation is required. Orimiechie et al. (2017) demonstrated temperature compensation by orientating two sets of FBG sensors 15° apart – the two having different sensitivity to strain, but the same sensitivity to temperature. Xiong et al. (2018) used a method by pasting two FBG sensors on opposite sides of the elastomer. This caused both positive and negative induced strain, resulting in opposite wavelength shifts, but identical temperature-induced shifts. Guo (2019) proposed super structure FBG sensors, consisting of long-period fiber grating (LPFG) written in the same fiber section to measure strain and temperature by measuring the change in peak wavelength (for strain) and in reflection power of the trough (for temperature) in the spectrum.

2.2 Distortions in FBG sensors

When FBG sensors are embedded between non-parallel fibers, this can induce torque on the FBGs, causing signal distortions, so loading types and orientation are important factors to consider. Kahandawa, Epaarachchi and Wang (2011) demonstrated the effect of loading type and fiber orientation on the signal. Applying lateral load to the specimens, the ones with fiber orientation not in parallel with the sensor experienced spectral distortion: they used an FBG fixed filter to capture spectral distortion, demonstrating that the area of the filtered spectrum captured by the photo detector was proportional to strain, allowing time domain data to be directly converted into strain.

2.3 Damage detection using FBG sensors

Okabe et al. (2007) looked at detection methods of transverse cracks using FBG sensors and demonstrated spectrum distortion when cracks began to form: peak intensity decreasing, and smaller peaks appearing around peak maximum. They concluded that full width at half maximum of the spectrum is indicator for real-time detection of transverse cracks in carbon fiber reinforced plastics. Cook, Alavija and Wildy (2017) proposed a governing differential equation for the behavior of thin beams to detect delamination damage. They conducted a cantilever bend test and a free vibration test on a damaged and undamaged carbon fiber specimen. They passed the measured signal through a Savitzky-Golay filter, demonstrating that wavelets formed in the FBG sensors in the region with the delamination. Yashiro et al. (2004) proposed a method of detecting and predicting multiple types of damages (splits, cracks, and delamination) in composite materials using finite element analysis, finding that splits and transverse cracks occur at lower strain levels, and delamination at higher strain levels growing from the splits and cracks. Leng and Asundi (2001) conducted a non-destructive 3-point bend test to evaluate damage, employing a force vs. micro-strain curve to demonstrate the results, indicating that flexural strain in damaged carbon fiber specimens was much higher than in the control specimens.

2.4 Interrogation in FBG sensors

Interrogation is the method to read the signal reflected from FBG sensors, and is conducted by shooting broadband light through the sensor and capturing the wavelengths of reflected light (Okabe, et al., 2007). Park et al. (2017) state that wavelength domain spectrum in passive interrogation systems based on amplified spontaneous emission (ASE) have a low signal to noise ratio and limited wavelength resolution, making them unsuitable for real-time dynamic measurements. They proposed a resonance Fourier domain mode locked (FDML) fiber laser for a high-speed dynamic measurement, and demonstrated that signals obtained in the time domain were in linear relationship with the wavelength domain signal, and could monitor in real-time abrupt change in frequencies applied to the sensor without any signal delay.

2.5 Data analysis using deep learning

Zhang and Wang (2020) utilized a deep CNN (DCNN) to predict damage state of I-shaped steel beams (data obtained from FBG sensors and accelerometers). They trained the CNN and validated through experimentation. They also employed model-based transfer learning (TL) to transfer the parameters of the CNN to a T-shaped reinforced concrete beam. This is important as retraining a NN for each scenario is time consuming and may be impractical. The accuracy of the CNN trained using the data sets was above 99%, demonstrating that a CNN can automatically extract features and identify damage types (Zhang & Wang, 2020); also, when transfer learning was utilized for the T-shaped concrete beam, the training process was three times faster compared to an untrained CNN.

3. SETUP EXPERIMENT

An experiment was conducted to test our FBG sensor and to produce meaningful signal response representing composite material condition, be used to design the experimental system, and as ground truth for NN training. The experiment was conducted in the Engineering Materials Laboratory of Griffith University. An ASTM 3-point bend and fracture test was conducted, with strain measured using FBGs (ASTM International, 2021). The experiment was repeated twice using pre-fractured specimen and control specimen made from unidirectional prepreg carbon fiber. The pre-fractured specimen had 45mm insert, simulating delamination damage.

Using an Instron Universal testing system and Bluehill Universal software, force and displacement measurements of the transducer were obtained (see Figs. 3 and 4a). A USB microscope was used to monitor fracture propagation to match features in video with the sensor data (see Fig. 4b).

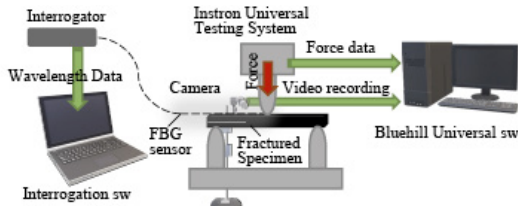


Figure 3. Experimental setup schematic diagram

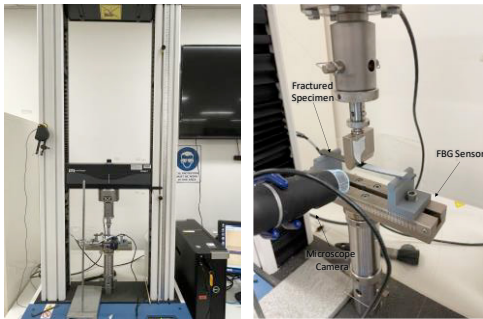


Figure 4. (a) Experimental setup (b) Experimental setup (Close up)

An FBG sensor was pasted onto the top surface of each specimen using masking tape; due to technical constraints only one FBG sensor was available thus permanently embedding the sensor into the specimen was not possible. The sensor used was a draw tower grating FBG with 6 elements. Grating locations are shown in Fig. 5.

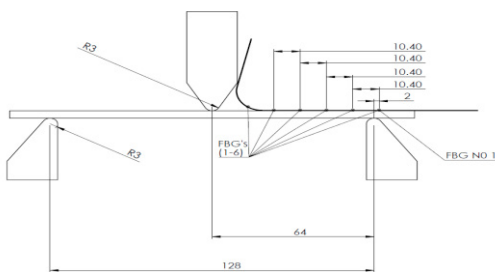


Figure 5. FBG placement on the specimen (units are in mm)

The FBG sensor was connected to an I-MON 256 USB interrogator, and monitored using a secondary computer. Using the I-MON evaluation software, time – wavelength data and spectral data (pixel – reflectivity) were obtained.

4. RESULTS AND DISCUSSION

Figure 6 is a photo of the fractured specimen after it failed. The marker (a) is where delamination was inserted and (b) is to where the crack propagated (after failure it was 85mm). Figures 7 & 8 show time vs. wavelength data (wavelength values at t=0 were aligned with the value at FBG1 to make the graph more informative). Figs. 6 & 7 show that signal wavelengths decrease with time (until failure).

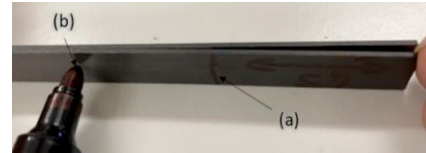


Figure 6. Failed fractured specimen

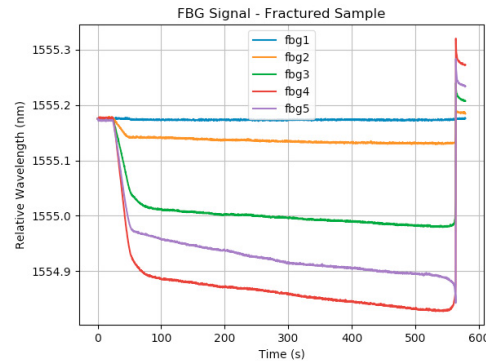


Figure 7. Fractured specimen, time-wavelength graph (values relative to FBG1)

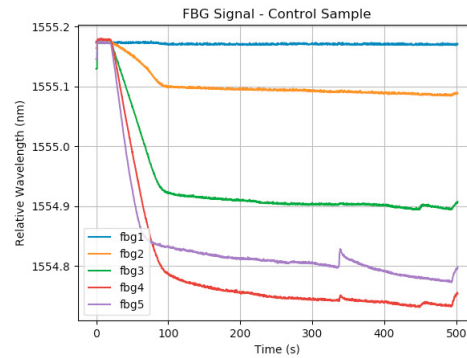


Figure 8. Control specimen, time-wavelength graph (values relative to FBG1)

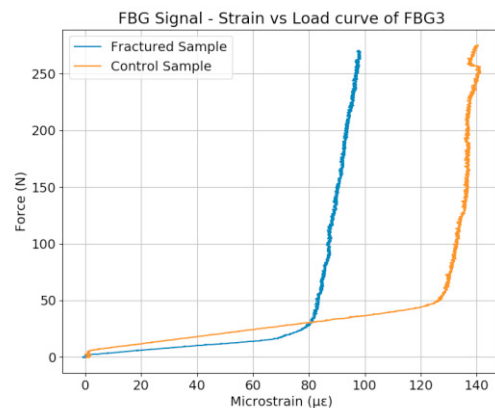


Figure 9. Strain-Force graph for FBG3

Normally reflected wavelength from an FBG sensor increases with strain, but in this experiment the sensor was placed on top of the specimen causing the fibre to constrict when applying force, thus the reverse response of the FBG sensor. Both Figs. 7 & 8, demonstrate that FBG1 experienced the least strain and the strain increased as the FBGs moved towards the center except for FBG4. The results indicate that the grating located around where FBG4 was located experiences the most strain (FBG1 retains a relatively straight signal as it was located outside of the supporting pins). In both specimens, at 20s mark, a steep wavelength decline can be observed, indicating the transducer beginning to apply force. With the fractured specimen, strain was induced until failure (see Fig. 6 at 564s), where the relative wavelength of all FBGs experienced a sudden rise. The signal at FBG5 shows a dip right before failure at 564s, demonstrating that the specimen at location FBG5 experienced a sudden increase in strain. It was observed that the length of the pre-made fracture increased suddenly, when the specimen made a snapping sound and failed, suggesting that sudden propagation of delamination caused increased strain at FBG5.

Figure 9 demonstrates the force-strain graph of FBG3. This graph type was used by Leng and Asundi (2001), and similarly to their results, the fractured specimen experienced higher strain levels until the intersection. However, the control specimen started to experience more strain at around $80\mu\epsilon$. In Leng and Asundi's experiment they were conducting non-destructive tests. As a result, it is likely that their specimen remained within the elastic limit unlike the experiment conducted in this project, where the fractured specimen was tested until failure, and the control specimen was exposed to the same force levels, thus it is highly likely that both specimens experienced plastic deformation. Furthermore, force N in the control specimen increases at a steady rate before the sudden rise, for longer than the fractured specimen. A possible explanation for this is that the low rise represents elastic deformation while the sudden rise represents plastic deformation. Due to the fractured specimen having a delamination insert causing it to have a lower stiffness, the control specimen was able to remain in the elastic range for longer than the fractured specimen.

The results suggest that the graphing method Leng and Asundi used can be used for damage detection in CFRPs while the part remains in the elastic region (Leng & Asundi, 2001). These results demonstrate that damage can be detected in composite materials using FBG sensors. However, in this proof-of-concept experiment conducted only one of each specimen was tested, therefore additional testing is required to statistically validate these results.

5. FUTURE EXPERIMENTAL SETUP

The objective of this paper is to propose a concept of an experimental setup which will allow future researchers to use experimentally obtained ground truth data so that using measured data from fiber Bragg grating sensors they can setup, experiment with, and design a structural health monitoring system for aerospace structures. In this Section the proposed system will be described in detail.

5.1 Damage detection and classification

The major advantage of CNNs is that feature extraction is automated. Ibrahim et al. (2020) demonstrated that a CNN was the best at classifying damage types within engineering materials compared to other techniques (such as Support vector machine, k-nearest neighbor algorithm and double integral + high-pass filter) despite using manual extracted features, while the CNN utilized only raw data. Zhang and Wang (2020) could utilize CNNs to monitor the health in engineering structures using FBG sensors, demonstrating a proof of concept, and could demonstrate that transfer learning can be applied to CNNs to speed up the training process for damage classification in irregular shaped specimens, complex damage modes and multi-axial loading. Farrah, Worden et al. (2012) demonstrated that time series data can be extracted in a simpler way compared to spectral data. Finotti et al. (2019) utilized an artificial neural network (ANN) and a support vector machine (SVM) to identify structural changes of a railway bridge using raw vibration data, demonstrating that the ANN had a mean accuracy of 87% compared to the 80% of the SVM (Finotti, et al., 2019), and claiming that this will allow dealing with dynamic data without needing to perform a model identification procedure. This method could be applied using FBG sensors, as FBG sensors are also able to measure vibration (Sahota, et al., 2020).

Lee et al. (2020) extracted 41 relevant sensing variables out of 186 from a black-box dataset and used a deep autoencoder (DAE) model to model the flight operation and detect precursors to aircraft upsets. They used a Savitzky-Golay filter and decimation to synchronize the sampling rate and size of the variables, which was used as ground truth for training the DAE model. The trained model was able to detect precursors to aircraft upset events with a maximum of 122s before stick shaking (Lee, et al., 2020). In addition, they demonstrated that CNNs can be used to demodulate overlapped signals and showed that they out-performed other machine learning techniques such as differential evolution (DE), long short-term memory (LSTM) and extreme learning machine (ELM), which will eventually become necessary in a highly multiplexed SHM system.

Regarding discrimination: there is more than one characterization that we may want to identify, such as classifying a state or classifying a trend:

- i) For each FBG (i.e., xyz location in the material), look at a snapshot of the dominant reflected frequency at any moment in time and discriminate between desirable and undesirable states, or possibly further classify the region of strain: elastic [desirable], plastic [undesirable] (with micro cracks having appeared), and broken [undesirable]).
- ii) For each FBG (i.e., xyz location in the material), look at the time series of snapshots of the dominant reflected frequency, and identify whether there is a trend in the change of strain leading to a drift from desirable to undesirable state.
- iii) For each FBG grating, based on the presence of peaks in the *spectrum* of the reflected light, identify state as per i).
- iv) Same as iii) but identify trend.

5.2 Testing methods

The types of physical tests to produce training data are an important factor to consider (including static and dynamic loads). During early testing phases, utilizing a tensile strength test to train the neural network is fundamental. This is because it applies strain on the specimen along a single axis, keeping other variables constant. Also, many researchers conducted tensile strength test for damage detection in composite materials using FBG sensors (Guo, 2019) (Kahandawa, et al., 2011) (Okabe, et al., 2007) (Yashiro, et al., 2004), and their results can be used as reference in early stages to compare and validate results of the experiments.

Alternatively, finite element analysis could be used to simulate the expected spectrum of FBG sensors, which then can be used to train the neural network. Yashiro et al. (2004) demonstrated that by combining finite element analysis and optical analysis, it is possible to predict the spectrum of the FBG sensor in damaged composites. In later stages, employing additional loading modes should be considered. If the neural network can classify the damage within the specimens, the model might be transferred to a similar but different loading type. E.g., Kahandawa et al. (2011) applied both axial and torsional load, showing that a slight modification to the tensile strain test can save effort.

The SHM system is to operate under unpredictable dynamic load, which is a reminder that most existing research on dynamic loading in CFRP only involved applying systematic sinusoidal load. In the final experimentation stages, a method to train the neural network to operate under chaotic dynamic load is necessary. Alam et al. (2019) suggest collecting real-life random spectral loading data and extrapolating it to a laboratory-testing regimen, which can be used to train the neural network.

5.3 FBG sensor placement

Eventually FBG sensors must be embedded in the specimen to be more sensitive to invisible interlaminar damages. However, embedding FBG sensors within the composite is not an easy task and is irreversible (Kahandawa, et al., 2012). Therefore, initial testing should use surface mounted FBGs to keep the sensors reusable for multiple experimentations. In later phases, embedded sensors should be considered. The cheapest method is the hand layup process of manually rolling the sensor onto the composite (Kahandawa, et al., 2012), however, this is time consuming and inconsistent in terms of precision. Another relatively cheap method is using a vacuum bag to seal the composite during the curing process. Although the quality is not as good as using an autoclave, the composite can be cured with much cheaper equipment (Kahandawa, et al., 2012). When conducting experiments on irregular-shaped specimens, a finite element analysis should be performed to predict sections within the specimen that have the highest strain concentration to inform sensor placement.

5.4 Temperature compensation

Due to temperature compensation difficulties in using FBG sensors, early-stage experiments should be conducted in a

laboratory to keep temperature constant. Xiong et al.'s (2018) method of pasting two FBG sensors on opposite sides of the elastomer is easy and can be used in early testing stages.

Ideally the super structure FBG proposed by Guo (2019) should be utilized for simultaneous measurement of strain and temperature, as this requires only 1 fiber and no additional material to be embedded. However, it requires a long period fiber grating to be written on top of a fiber Bragg grating, requiring additional equipment. Also, this has only been validated in temperature range of 20°C to 100°C (Guo, 2019), which is not within the boundary to which aerospace structures are exposed, therefore further testing is necessary to validate this method within the desired temperature range.

5.5 Interrogation systems

In this project, the I-MON 256 USB interrogator was used to measure the wavelength data of the FBG sensor. Park et al. (2017) stated that interrogation methods that obtain wavelength domain data from an ASE light source has a low signal to noise ratio and has low wavelength resolution. Park et al.'s (2017) method of using a modified Fourier domain mode locked (FDML) fibre laser with FBG sensors inscribed in the wiring is great at high-speed monitoring of spectral data in the time-domain. Although Park et al (2017) claimed that this technique had potential for use in SHM, the FDML technique requires a long signal delay line to synchronize the roundtrip time with the filter tuning frequency. Alternatively, Kanhandawa et al.'s (2011) method of using a fixed FBG filter could be used: due to its ability to monitor the spectrum in real time; speed and accuracy could be verified through experimentation and evaluated for aerospace application.

6. CONCLUSIONS AND FURTHER WORK

Our objective was to analyze the requirements and propose an experimental setup for SHM of aerospace structures using FBG sensors. This setup is planned to be used to generate training data for the feature identification NN component of the system. The analysis included reviewing literature on using FBG sensors for structural health monitoring, conducting an experiment using the FBG sensors, and using this information to inform the design of our future SHM system. A neural network was proposed for damage identification and classification as neural networks can automatically extract features. It was demonstrated that time domain data can be used to detect structural changes in real time. Furthermore, Lee et al. (2020) were able to detect precursors of aircraft upset events from a black-box dataset using a neural network. Utilizing a CNN in similar experiments may produce interesting results as CNNs require less computational power than fully connected neural networks and it was demonstrated that CNNs produced the most accurate results compared to other techniques (Ibrahim, et al., 2020). To classify states and trends in each sample (healthy, damaged, broken), more than one CNN would be needed (potentially at least four) using snapshots of dominant reflected frequency and spectra of the reflected light.

The results of the experiment demonstrated that it was possible to use FBG sensors to discriminate between damaged and undamaged composite materials. However, the

results were not statistically significant due to the limited number of test specimens. In future stages of this project, repeated tests of an estimated minimum of 5 specimens (of each type) should be conducted to obtain statistically significant data. Additional experiments involving multiple loading modes such as tensile strength test, cantilever beam test, multi-axial loading and cyclic loading are required to produce ground truth data for a neural network that can detect various types of damages under complex loading conditions.

7. ACKNOWLEDGEMENTS

The support of Associate Professor Wayne Hall and Dr Ian Underhill with advice, production of specimens and experimental setup are gratefully acknowledged.

REFERENCES

- Alam, P., Mamalis, C., Floerani, C. & O Bradaigh, C. M. (2019). The fatigue of carbon fibre reinforced plastics - A review, *Composite Part B: Engineering*, Vol.166:555-579.
- ASTM International (2021). ASTM D7264-21, Standard Test Method for Flexural Properties of Polymer Matrix Composite Materials, West Conshohocken: American Society for Testing and Materials.
- ASTM International (2021). ASTM D7905M-14, Standard Test Method for Determination of the Mode II Interlaminar Fracture Toughness of Unidirectional Fiber-Reinforced Polymer Matrix Composites, West Conshohocken: American Soc. for Testing and Materials.
- Cook, P. R., Alavija, A. & Wildy, S. J. (2017). Identification and Characterisation of Delamination Damage in Composites utilising Embedded Optical Strain Gauges. 9th Aus. Congress on Applied Mechanics, pp140-147.
- Department of Defense (2008). Condition-based maintenance plus DoD guidebook. Washington, USDoD
- Derriso, M. M., McCurry, C. D. & Schubert Kabban, C. M. (2016). A novel approach for implementing structural health monitoring systems for aerospace structures. In: F. G. Yuan (ed.) *Structural Health Monitoring (SHM) in Aerospace Structures*. Amsterdam: Elsevier, pp. 33-56.
- Farrar, C. R. & Worden, K. (2012). *Structural Health Monitoring A Machine Learning Perspective*. Wiley.
- Finotti, R. P., Cury, A. A. & Barbosa, F. S. (2019). An SHM approach using machine learning and statistical indicators extracted from raw dynamic measurements. *Lat. Am. J. Solids Struct.* 16(2):1-17
- Giurgiutiu, V. (2014). In: V. Giurgiutiu, ed. *Structural Health Monitoring with Piezoelectric Wafer Active Sensors (Second Ed.)*, Academic Press, pp.1-19.
- Guo, G. (2019). Superstructure fiber Bragg gratings for simultaneous temperature and strain measurement. *Optik*, Vol.182:331-340.
- Ibrahim, A., Eltawil, A., Na, Y. & El-Tawil, S. (2020). A Machine Learning Approach for Structural Health Monitoring Using Noisy Data Sets. *IEEE Trans. Autom. Sci. Eng.*, 17(2):900-908.
- Kahandawa, G. C., Epaarachchi, J. & Wang, H. (2011). Identification of Distortions to FBG Spectrum Using FBG Fixed Filters, In Proc. 18th ICCM, Korean Society for Composite Materials.
- Kahandawa, G. C., Epaarachchi, J., Wang, H. & Lau, K. T. (2012). Use of FBG Sensors for SHM in Aerospace Structures. *Photonic Sensors*, 2(3):203-214.
- Kusiak, A. (2019). Convolutional and generative adversarial neural networks in manufacturing. *Int. J. Prod. Res.*, 58(5):1594-1604.
- Lee, H., Lim, H. J. & Chattopadhyay, A. (2020). Data-driven system health monitoring technique using autoencoder for the safety management of commercial aircraft. *Neural. Comput. Appl.*, Vol.33:3235–3250.
- Leng, J. S. & Asundi, A. (2001). Non-destructive evaluation of smart materials by using extrinsic Fabry-Perot interferometric and fiber Bragg grating sensors. *NDT E Int.*, 35(4):273-276.
- Okabe, Y., Yashiro, S., Kosaka, T. & Takeda, N. (2007). Detection of transverse cracks in CFRP composites using embedded fiber Bragg grating sensors. *Smart Mater. Struct.* Vol.9:832-838.
- Oromiehie, E., Prusty, B., Compston, P. P. & Rajan, G. (2017). in-situ simultaneous measurement of strain and temperature in automated fiber placement (AFP) using optical fiber Bragg grating (FBG) sensors. *Adv. Manuf.: Polym. Compos. Sci.*, 3(2):52-61.
- Pai, A. (2020). CNN vs. RNN vs. ANN – Analyzing 3 Types of Neural Networks in Deep Learning. [Online] <https://www.analyticsvidhya.com/blog/2020/02/cnn-vs-rnn-vs-mlp-analyzing-3-types-of-neural-networks-in-deep-learning/>
- Park, J., Kwon, Y. S., Ko, M. O. & Jeon, Y. (2017). Dynamic fiber Bragg grating strain sensor interrogation with real-time measurement. *Opt. Fiber Technol.*, Vol.38:147-153.
- Sahota, J. K., Gupta, N. & Dhawan, D. (2020). Fiber Bragg grating sensors for monitoring of physical parameters: a comprehensive review. *Opt. Eng.*, 59(6):1-35.
- Tian, K., Liu, Y. & Wang, Q. (2005). Temperature-independent fiber Bragg grating strain sensor using bimetal cantilever. *Opt. Fiber Technol.*, 11(4):370-377.
- Werneck, M.M., Allil, B.A., & Nazaré, F.V. (2013). A Guide to Fiber Bragg Grating Sensors. In: C. Cuadrado-Laborde (ed). *Current Trends in Short- and Long-period Fiber Gratings*. pp1-24 Intech. doi.org/10.5772/54682
- Xiong, L. et al. (2018). Investigation of the Temperature Compensation of FBGs Encapsulated with Different Methods and Subjected to Different Temperature Change Rates, *J. Light. Technol.*, 37(3):917-926.
- Yashiro, S., Takeda, N., Okabe, T. & Sekine, H. (2004). A new approach to predicting multiple damage states in composite laminates with embedded FBG sensors. *Compos Sci Technol*, 65(3-4):659-667.
- Zhang, W. & Wang, D. (2020). Damage identification using deep learning and long-gauge fiber Bragg grating sensors. *Appl. Opt.*, 59(33):10532-10540.